Lukas Nejdl[1,2]
Hoai Viet Nguyen[1,2]
Lukas Richtera[1,2]
Sona Krizkova[1,2]
Roman Guran[1,2]
Michal Masarik[3]
David Hynek[1,2]
Zbynek Heger[1,2]
Karin Lundberg[4]
Kristofer Erikson[4,5]
Vojtech Adam[1,2]
Rene Kizek[1,2]

[1]Central European Institute of Technology, Brno University of Technology, Brno, Czech Republic
[2]Department of Chemistry and Biochemistry, Mendel University in Brno, Brno, Czech Republic
[3]Department of Pathological Physiology, Faculty of Medicine, Masaryk University, Brno, Czech Republic
[4]Lab on a Bead AB, Division of Research and Development, Uppsala, Sweden
[5]Department of Engineering Sciences, Division of Solid State Physics, The Ångström Laboratory, Uppsala University, Uppsala, Sweden

Received February 5, 2015
Revised May 6, 2015
Accepted May 9, 2015

Research Article

Label-free bead-based metallothionein electrochemical immunosensor

A novel microfluidic label-free bead-based metallothionein immunosensors was designed. To the surface of superparamagnetic agarose beads coated with protein A, polyclonal chicken IgY specifically recognizing metallothionein (MT) were immobilized via rabbit IgG. The Brdicka reaction was used for metallothionein detection in a microfluidic printed 3D chip. The assembled chip consisted of a single copper wire coated with a thin layer of amalgam as working electrode. Optimization of MT detection using designed microfluidic chip was performed in stationary system as well as in the flow arrangement at various flow rates (0–1800 μL/min). In stationary arrangement it is possible to detect MT concentrations up to 30 ng/mL level, flow arrangement allows reliable detection of even lower concentration (12.5 ng/mL). The assembled miniature flow chip was subsequently tested for the detection of MT elevated levels (at approx. level 100 μg/mL) in samples of patients with cancer. The stability of constructed device for metallothionein detection in flow arrangement was found to be several days without any maintenance needed.

Keywords:
Immunosensor / Label-free / Metallothionein / Superparamagnetic particles
DOI 10.1002/elps.201500069

1 Introduction

Metallothioneins (MT) are cysteine-rich heavy metal-binding proteins, which are ubiquitous from bacteria to animals [1]. In spite of the fact that there are differences in their structures, they exhibit a high degree of structural homology. Mammalian MTs are of 61 or 62 amino acid polypeptides containing 20 conserved cysteine residues that underpin the binding of metals. Four MT isoforms (MT-1, MT-2, MT-3, and MT-4) have been found so far, but these have also subtypes with 17 MT genes identified in human, of which ten are known to be functional. Different cells express different MT isoforms with varying levels of expression probably as a result of the different function of each isoform, however, these remain unclear [2, 3]. In human, this protein is most frequently studied in connection with heavy metals homeostasis and detoxification, oxidative stress, and some pathological processes [4, 5].

Metallothioneins manifest varying expression levels in carcinomas, and they may be considered as valuable cell cancerization biomarkers for diagnosis of oncopatients [6]. The increased expression of MT at protein level has been found at spinocellular carcinoma [7], solid childhood tumors [8], head and neck tumors [9], hepatocellular carcinoma [10], and others [11–13]. Moreover, lower expression of MT in various benign tumor tissues than that in corresponding malignant tumors has been found in several studies summarized by Gumulec et al. in their metaanalysis [14]. MT expression difference is associated with various stages of tumor in cancer patients and could be an useful clinical criterion of distinguishing benign tumors and malignant tumors [6, 14]. Moreover, MT interacting with other proteins (ferritins, transcription

Correspondence: Professor Rene Kizek, Department of Chemistry and Biochemistry, Mendel University in Brno, Zemedelska 1, CZ-613 00 Brno, Czech Republic
E-mail: kizek@sci.muni.cz
Fax: +420-5-4521-2044

Abbreviations: CV, cyclic voltammetry; **DPV**, differential pulse voltammetry; **HMDE**, hanging mercury drop electrode; **MT**, metallothioneins; **PAMB**, protein A agarose magnetic bead; **SAE**, solid amalgam electrode; **WE**, working electrode

Colour Online: See the article online to view Figs. 1–6 in colour

factors, metalloenzymes, endocytic receptors, etc.), low-molecular mass compounds and heavy metals control the redox processes and regulation of gene expression [15]. In tumour cells, these functions affect the resistance of a tumor to cytostatics, and lead to insensitivity to proapoptotic signals [16].

In biological tissues MT is most frequently determined by immunoanalysis and electrochemical techniques [17]. Electrochemical methods using hanging mercury drop electrode (HMDE) and Brdicka reaction are generally the most sensitive techniques for MT detection [18–22]. The limited mechanical endurance and relative constructional complexity of HMDE are one of most substantial problems for establishing this type electrode to portable analysers and use "in field" instruments for large-scale inexpensive monitoring of various chemical species. Flow-through techniques where the use of liquid mercury is also unfeasible represent another issue. For these reasons, new types of solid electrodes have been introduced during the last decades and development of further alternatives is still the focus of many electroanalytical studies. Solid amalgam electrodes (SAE) represent electrochemically most similar alternative to mercury electrodes and it combines advantages of both types [23–25]. SAE electrodes can work with actually solid amalgam surface, or can be modified with mercury meniscus or thin electrolytically deposited mercury film [24–34]. For MT as an analyte several sensors, biosensors, immunosensors, and nanosensors employing miscellaneous labels or label-free sensors have been developed as QCM immunosensors [35–37] or colorimetric detection using a thymine-rich oligonucleotide-Hg complex and gold nanoparticles [38], FRET, potentiometric electrode for isoform-selective biosensing of MT [39]. From these, sensitive electrochemical immunoassay of MT-3 using carbon dots/Nafion film for antibody immobilization and $K_3[Fe(CN)_6]$ as a redox-active signal has been reported [40]. Table 1 is summarizing the major advantages and disadvantages of selected electrochemical methods for determination of MT.

Currently, a massive development of chip and/or microfluidic methods employing paramagnetic particles is experienced. These methods are advantageous for analyte separation from a sample and automated sample handling and analysis in immunoassays, either as mobile substrates on which the target antigen is captured, as detection labels, or simultaneously as substrates and labels. This has an application for detection of antibodies, disease biomarkers in serum or biotoxins from food samples. Several of the most sensitive assays allow protein detection down to fg/mL concentrations [41–45].

In our work, we suggested a label-free microfluidic paramagnetic bead-based immunosensor for MT employing previously characterized chicken anti-MT antibodies [46]. The conditions of electrochemical analyses were optimized in detail and amalgam working electrode was integrated into 3D printed fluidic platform, which achieved better sensitivity than commonly utilized stationary arrangement.

2 Materials and methods

2.1 Chemicals

All chemicals used in this study were purchased from Sigma Aldrich (St. Louis, MO, USA) in ACS purity unless noted otherwise. Pipetting was performed by pipettes from Eppendorf (Hamburg, Germany). High purity deionized water (Milli-Q Millipore 18.2 MΩ/cm, MA, USA) was used throughout the study. MT was isolated from rabbit liver and purified by using fast-protein liquid chromatography according to our previous study [47]. The purity was evaluated by using MALDI-TOF/TOF (Bruker ultrafleXtreme, Bruker Daltonik GmbH, Germany). As a standard, rabbit MT (mixture of MT-1 and -2, Ikzus Proteomics, Genova, Italy) was used. Protein A UltraRapid Agarose developed by Lab on a Bead AB (Uppsala, Sweden) was kindly provided by them for this study. Protein A UltraRapid Agarose consists of super-paramagnetic agarose beads covalently coupled with recombinant protein A.

2.2 Chicken yolk anti-MT antibodies

Two chickens were immunized with MT and IgY fractions with reactivity to MT were collected from the egg yolk. The obtained IgY were purified by immunoaffinity chromatography and final concentration of proteins was established to 54.7 mg/mL. The antibodies in PBS were stabilized with 0.1% sodium azide *w/w*. The immunoreactivity of produced antibodies was tested in our previous studies [48, 49]. The entire process was conducted in accordance with the Regulations for the Care and Use of Laboratory Animals (311/1997, Ministry of Agriculture, Czech Republic).

Table 1. Major advantages and disadvantages of selected electrochemical methods for MT determination

Electrode	Type	RSD	Advantages	Disadvantages	Reference
Amalgam	Electrochemistry (F)	8%	Cheap and fast preparation	Cannot be stored	This article
Glassy carbon	Electrochemistry (F)	2%	Small amount of analyte can be used	Only for amperometric measurements	[62]
-	EQCM (F)	1–3%	Small amount of analyte can be used	Complicated instrumentation	[63]
CCPE	Electrochemistry (S)	NS	Nontoxic material	Difficult miniaturization and preparation	[64]
HMDE	Electrochemistry (S)	5%	Ane measurement, one drop	Toxic material	[65]

F, flow through mode; S, stationary mode; EQCM, electrochemical quartz crystal microbalance; CCPE, carbon composite paste electrode; HMDE, hanging mercury drop electrode.

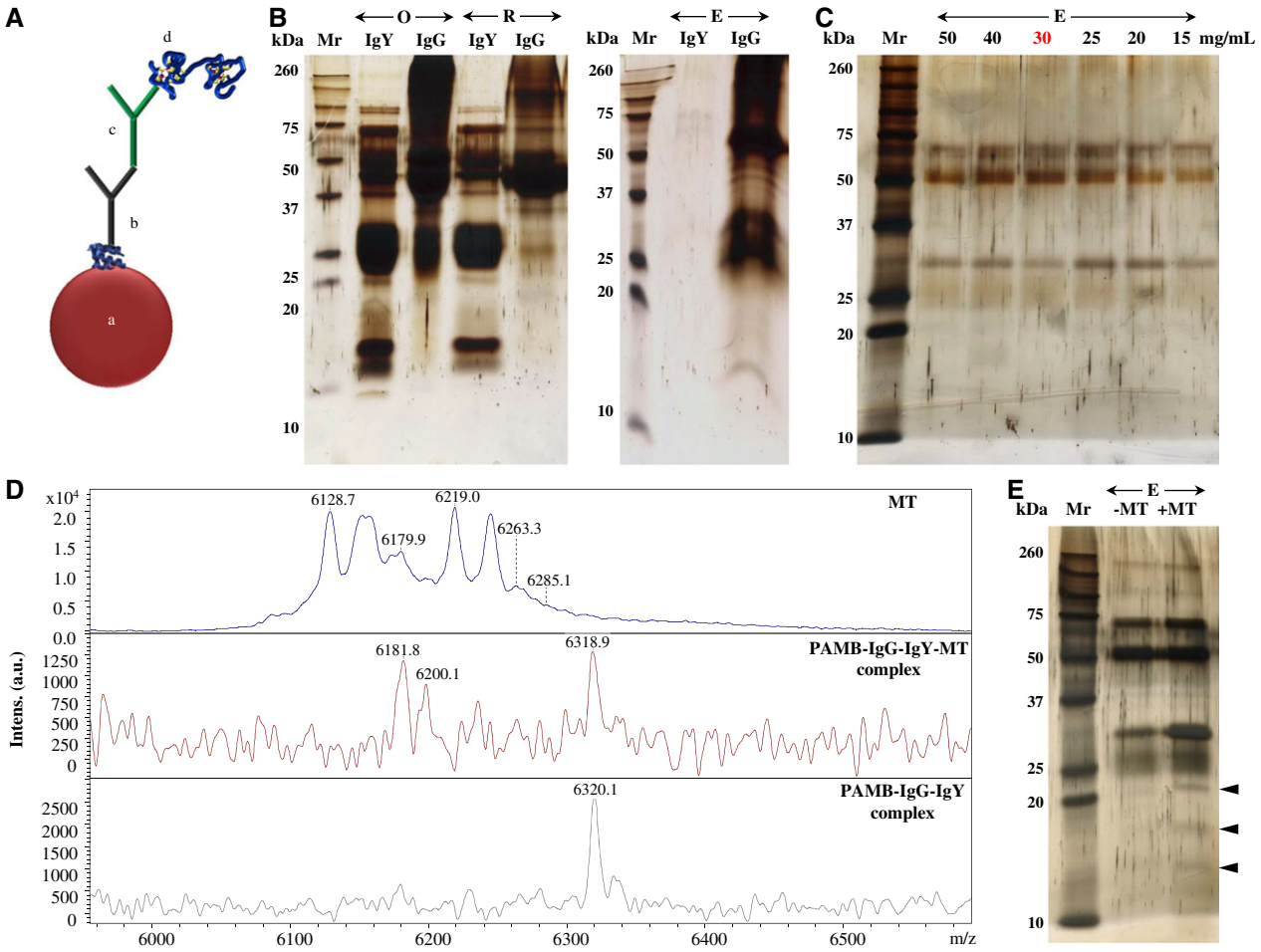

Figure 1. Construction and verification of the immunosensor. (A) Structure of the PAMB-IgG-IgY-MT immunocomplex. (a—Protein A agarose bead (PAMB), b—Rabbit anti-chicken IgY (IgG), c—Chicken anti-MT (IgY), d—Metallothionein (MT)). (B) Comparison of IgG and IgY binding to the beads O – original sample, R – retented proteins, E – eluted antibody. (C) Determination of the beads capacity for rabbit IgG. E – eluted antibody. The capacity of the beads was estimated to be between 23.1 and 27.8 mg per mg of the beads. For further experiments the beads were coated with 27.8 mg IgG per mg of the beads (highlighted with red). (D) MALDI spectra of MT standard, PAMB coated with antibodies with captured MT standard (PAMB-IgG-IgY-MT complex) and PAMB coated with antibodies without MT (PAMB-IgG-IgY complex). (E) Comparison of protein profiles eluted from PAMB coated with antibodies with and without MT standard. Arrows indicate additional bands in PAMB-IgG-IgY-MT.

2.3 Modification of the paramagnetic beads with antibodies

For immunosensor construction (Fig. 1A), the protein A agarose magnetic beads (PAMB) were coated with rabbit IgG raised anti chicken IgY (Sigma-Aldrich, St. Louis, MO, USA) in concentration of 30 mg per 1 mL of settled beads, i.e. 27.8 mg per mg of the beads. The coating was carried out in 15 mM PBS pH 7.4 with 150 mM NaCl at 25°C for 60 min on a rotator (Multi RS 60, Biosan, Riga, Latvia). After the incubation the solution was removed and the beads were washed twice with two times higher sample volume of washing buffer (15 mM PBS pH 7.4 with 150 mM NaCl), 55.6 mg of IgY per mg of the beads was added and the beads were incubated on a rotator at 25°C for additional 60 min. Then, the solution was removed and the beads were washed twice in three times higher sample volume with washing buffer, resuspended in original volume of binding buffer and immediately used for further experiments.

2.4 Metallothionein binding to the immunosensor

For one analysis 10 μL of the sample and 2 μL of the beads was mixed, the total volume was filled up to 50 μL and the sample was incubated at 25°C for 60 min on a rotator (Multi RS 60, Biosan, Riga, Latvia). Then, the solution was removed, the beads were washed twice in three times higher sample volume with washing buffer, resuspended in original volume of binding buffer and used for further analysis.

2.5 SDS-PAGE

The electrophoresis was performed according to Laemmli [50] using a Mini Protean Tetra apparatus with gel

dimension of 8.3 × 7.3 cm (Bio-Rad, USA). First 12.5% *w/v* running, then 5% *w/v* stacking gel was poured. The gels were prepared from 30% *w/v* acrylamide stock solution with 1% *w/v* bisacrylamide. The polymerization of the running or stacking gels was carried out at room temperature for 45 min or 30 min, respectively.

For electrophoretic analysis the proteins were eluted from the beads with 10 μL of 50 mM glycine, pH 2.5 at 25°C for 15 min under rotation (Multi RS 60, Biosan, Riga, Latvia). Then, the samples were mixed with reducing sample buffer (3% β-mercaptoethanol) in a 2:1 ratio. The samples were boiled for 3 min, and the sample was loaded onto a gel. For determination of the molecular mass, the protein ladder "Precision plus protein standards" from Biorad was used. The electrophoresis was run at 120 V for 70 min (Power Basic, Bio-rad USA) in tris-glycine buffer (0.025 M Trizma-base, 0.19 M glycine and 3.5 mM SDS, pH = 8.3). Then the gels were stained Coomassie-blue and consequently with silver [51].

2.6 MALDI-TOF/TOF MS

The experiments were performed using MALDI-TOF/TOF mass spectrometer Bruker Ultraflextreme (Bruker Daltonik GmbH, Bremen, Germany) equipped with a laser operating at wavelength of 355 nm with an accelerating voltage of 25 kV, cooled with nitrogen and a maximum energy of 43.2 μJ with repetition rate 2000 Hz in linear and positive mode, and with software FlexControl version 3.4 and FlexAnalysis version 2.2 for data acquisition and processing of mass spectra, respectively. Prior to analysis the beads were washed with three times higher sample volume of water and resuspended in 1% TFA *w/w*. The matrix (α-cyano-4-hydroxycinnamic acid—HCCA, in concentration 20 mg/mL) was prepared in TA30 (30% acetonitrile, 2.5% trifluoroacetic acid solution, w/w). The solutions for analysis were mixed in ratio of 1:1 (matrix/substance). After the obtaining a homogeneous solution, 1 μL was applied on the target and dried under atmospheric pressure and ambient temperature. A mixture of peptides calibrations standard (Bruker Daltonik GmbH, Bremen, Germany) was used for external calibration of the instrument. One MS spectrum was acquired by averaging 2500 subspectra (Smartbeam 2. Version: 1_0_38.5).

2.7 Determination of MT using HMDE

Determination of MT by differential pulse voltammetry (DPV) was performed with 663 VA Computrace instrument (Metrohm, Switzerland), using a standard cell with three electrodes. A HMDE with a drop area of 0.4 mm^2 was employed as the working electrode. An Ag/AgCl/3M KCl electrode was used as the reference and glassy carbon electrode served as auxiliary. For data processing 663 VA Computrace software from Metrohm CH was employed. The analysed samples were deoxygenated prior to measurements by purging with argon (99.999%). The Brdicka supporting electrolyte containing 1 mM $[Co(NH_3)_6]Cl_3$ and 1 M ammonia buffer (NH_3(aq) + NH_4Cl, pH = 9.6) was used. The supporting electrolyte was exchanged after each analysis. The parameters of the measurement by differential pulse voltammetry were as follows: initial potential of -0.7 V, end potential -1.8 V, deoxygenating with argon 90 s, deposition 120 s, time interval 0.2 s, step potential 1.95 mV, modulation amplitude 25.05 mV, and modulation time 0.57 s. For electrochemical measurement the volume of injected sample was 10 μL and volume of measurement cell 2 mL (10 μL of sample + 1990 μL ammonium buffer). Peak heights were measured from linear baseline (tangent to the curve joining beginning and end of the given peak). All measurements were carried out at 6 ± 1°C.

2.8 Determination of MT using Hg/Cu-WE and GCE

Electrochemical detection was performed using a three electrode system. Changes in the catalytic signal were recorded with a PGSTAT 101 potentiostat (Metrohm, Herisau, Switzerland) and the results were evaluated by the NOVA 1.8 software (Metrohm). Electrochemical determination was carried out by DPV and cyclic voltammetry (CV) in the Brdicka supporting electrolyte (see above) was used. The parameters of the measurement (DPV) were as follows: initial potential of –0.7 V, end potential of –1.5 V, modulation time 0.057 s, interval time 0.2 s, step potential –0.005 V, and modulation amplitude 0.025 V. CV was used as a cleaning step (Recovery surface Hg/Cu-WE) between the measurements, unless otherwise indicated. Parameters are follows: start potential –1.0 V, upper vertex potential –0.7 V, lower vertex potential –1.8 V, stop potential –1.0 V, cycles 60, step potential 2.4 mV and scan rate 0.4 V/s. Temperature (6°C) was controlled with a Peltier thermostat (Analytik Jena, Jena, Germany).

2.8.1 Modification of GCE with mercury

Modification of glassy carbon electrode were performed by inserting the electrode into 0.01 M $Hg(NO_3)_2$ solution prepared by the dissolution of 0.086 g mercury(II) nitrate in 25 mL of acidified (5% HNO_3, v/v) Milli-Q water. The potential (–0.9 V) was applied to the electrodes for 60 s, which resulted in the formation of a thin-film of mercury on the surface of the working electrode. The parameters of the measurement by differential pulse voltammetry were as follows: initial potential of –0.7 V, end potential –1.8 V, deposition 120 s, time interval 0.2 s, step potential 1.95 mV, modulation amplitude 25.05 mV, and modulation time 0.57 s. The Brdicka supporting electrolyte (see above) was used. The supporting electrolyte was exchanged after each analysis.

2.8.2 Modification of electrolytic copper wire as working electrode (Hg/Cu-WE)

Copper wires (Thermo scientific, Cambridge, UK) were used as working electrodes after modification. The copper was

were inserted into 0.01 M $Hg(NO_3)_2$ solution, prepared by the dissolution of 0.086 g mercury(II) nitrate in 25 mL of acidified (5% HNO_3, v/v) Milli-Q water. The electrodes were immersed in this solution for 10 min, which resulted in the formation of a thin-film of amalgam on the surface.

2.8.3 Stationary detection of metallothionein

Solid Hg/Cu-WE electrode with dimensions of 0.3 (diameter) × 20 mm (length) was used. An Ag/AgCl/3 M KCl electrode was the reference and platinum electrode was auxiliary. A sample (10 μL) of MT was pipetted into an electrochemical cell and then the electrolyte (2390 μL) was added. As an electrochemical cell, plastic UV/VIS semi-micro cuvette with dimensions 12.5 × 12.5 × 45 mm (Brand, Wertheim, Germany) was used. The electrode holder was printed by a PROFI 3D MARKER printing system (3Dfactories, Straznice, Czech Republic).

2.9 X-ray fluorescence

X-ray fluorescence was performed for elemental analysis of electrodes and was carried out Spectro Xepos (Spectro Analytical Instruments, Kleve, Germany). The sample was measured on a Pd anode X-ray tube working at a voltage of 47.63 kV and a current of 0.5 mA and detected with Barkla scatter aluminium oxide. Measurement time was 300 s. For excitation, Mo secondary target was used. The excitation geometry was 90º.

2.10 Scanning electron microscopy

Structure of electrodes was characterized by SEM. For documentation of the structure a MIRA3 LMU (Tescan, Brno, Czech Republic) was used. The SEM was fitted with In-Beam SE detector. For automated acquisition of selected areas a TESCAN proprietary software tool called Image Snapper was used. The software enabled automatic acquisition of selected areas with defined resolution. An accelerating voltage of 15 kV and beam currents about 1 nA gave satisfactory results.

2.11 Fluidic detection of metallothionein

Solid Hg/Cu-WE electrode with dimensions of 0.3 (diameter) × 8 mm (length) was used. The pipette tips (1 mL) made from polymeric material and coated by graphite were purchased from Tosoh Corporation (Tokyo, Japan) and were used as a reference and auxiliary electrodes. The reaction zone was designed for 150 μL of sample. The samples were injected using a peristaltic pump (Amersham Biosciences, Glattbrugg, Sweden).

2.12 Human serum samples

For purpose of testing of developed microfluidic device, serum samples from patients suffering from spinocellular carcinoma ($n = 3$), obtained from St. Anne´s University Hospital, Department of Otorhinolaryngology and Head and Neck Surgery, were used. Average age of patients was 56.7 years. Enlistment of patients into realized clinical study was approved by the Ethic committee of the Faculty of Medicine, Masaryk University, Brno, Czech Republic. The samples preparation prior to analysis was as follows: 10 μL of blood serum was mixed with 990 μL of 0.1 M phosphate buffer (pH 7.0), denatured at 99°C for 20 min in a thermomixer (Eppendorf 5430, Hamburg, Germany) and centrifuged for 10 min (Eppendorf 5402, Hamburg, Germany) to remove high-abundant proteins and peptides.

3 Results and discussion

3.1 Preparation of antibody-modified paramagnetic beads for MT binding

Primarily, the anti-MT antibody was bound to the beads surface. Due to the fact that IgY does not bind or bind only weakly to protein A/G, as it is obvious from Fig. 1B, where neither binding nor elution of IgY was observed, rabbit IgG raised anti chicken IgY, which bound well to beads surface (Fig. 1B), were used to capture the antibody. The capacity of the beads for rabbit IgG determined by SDS-PAGE was found to be within the range from 23.1 to 27.8 mg per mg of the beads (Fig. 1C). For further experiments the beads were coated with 27.8 mg IgG per mg of the beads, which was sufficient for complete coating of the beads with the antibody. In following step the beads were covered with 55.6 mg IgY per mg of the beads, which corresponds to two time higher molar beads capacity for IgY. Resulting beads-antibodies complex (PAMB-IgG-IgY) was used for further experiments.

Binding of MT to the immunosensor was verified by MALDI-TOF (Fig. 1D) and SDS-PAGE (Fig. 1E). Compared to PAMB-IgG-IgY, in MALDI-TOF MS spectrum of PAMB-IgG-IgY-MT, two additional peaks with identical localizations as at MT standard (mixture of rabbit MT 1 and 2 isoforms) were observed (m/z of 6181 and 6200 corresponding to isoforms MT 2D and 2E, respectively [52]). At the same time, after SDS-PAGE three additional bands in sizes of approximately 12, 18, and 24 kDa were observed at PAMB-IgG-IgY-MT complex, which corresponds to MT di-, tri-, or tetramers. Due to the tendency of MT to form oligomers under SDS-PAGE conditions [53] and due the low resolution of SDS-PAGE for low-molecular mass proteins, no band in size of MT monomer were observed.

These data indicate that MT was bound to the PAM-IgG-IgY surface in amount detectable with electrophoresis and therefore it was usable for further application in microfluidic immunosensor.

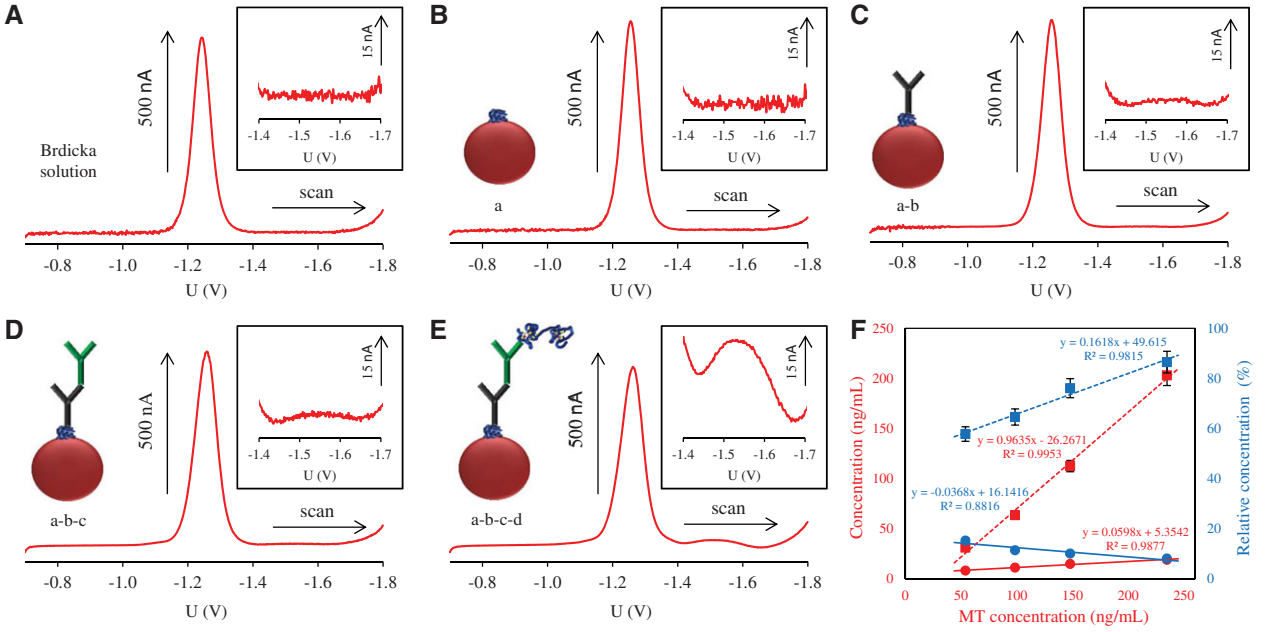

Figure 2. Differential pulse voltammetry of PAMB-IgG-IgY-MT complex and its building blocks. (A) DP voltammogram of Brdicka solution. (B) DP voltammogram of a = Protein A agarose bead (PAMB). (C) DP voltammogram of a-b = Protein A agarose bead (PAMB) with bonded Rabbit anti-chicken IgY (IgG). (D) DP voltammogram of a-b-c = Protein A agarose bead (PAMB) with bonded Rabbit anti-chicken IgY (IgG) and Chicken anti-MT (IgY). (E) DP voltammogram of a-b-c-d = complete PAMB-IgG-IgY-MT complex. (F) Dependence of used MT concentration on bonded and unbound MT (absolute concentrations – red lines, relative concentrations – blue lines, bonded MT – circles and solid line, nonbonded MT – squares and broken line). In insets (A–E): evaluated region from –1.4 V to –1.7 V and the Cat2 signal progression.

The possibility of MT detection bound in PAMB-IgG-IgY-MT complex was verified electrochemically by DPV using HMDE while the height of Cat2 signal of MT in Brdicka solution was evaluated [54]. Electrochemical methods especially in connection with the hanging mercury drop electrode are the most commonly used for determination of MT by Brdicka reaction. Brdicka reaction is electrochemical method for MT determination in biological samples [54–56]. Briefly, the reaction is based on the interaction of hexaamminecobalt(III) chloride complex ($[Co(NH_3)_6]Cl_3$) with protein containing –SH group [57]. The height of the last signal (Cat2) of Brdicka reaction voltammogram of real sample depends on the MT concentration [54]. RS2Co and Cat1 are other typical signals for Brdicka detection of MT [47, 51]. Full mechanism of the Brdicka catalytic reaction is still not fully understood, but the current knowledge was published by Raspor et al. [19, 58].

In order to exclude possible influence of individual building blocks of PAMB-IgG-IgY-MT complex all of its incremental building blocks were subjected to electrochemical determination separately (Fig. 2A–E). In each case, 10 μL of sample was dosed to 1.99 mL of the electrolyte (Brdicka solution) and a height of signal within the range from –1.4 V to –1.8 V, which corresponds to the region of Cat2 response (Fig. 2A–E), was monitored. This Cat2 signal corresponds to the electrochemical response of cysteine sulfhydryl groups and therefore very low signal can be usually observed even for all proteins bearing –SH groups. In the presence of MT (cysteine-rich proteins) this signal becomes to be significantly higher and can be used for quantitative detection of MT [59]. In accordance with this, the absence of Cat2 signal in the case of pure electrolyte and in the case of protein A magnetic agarose bead abbreviated as PAMB (Fig. 2A, B) is evident in DPV voltammograms.

Voltammogram of sample with PAMB is not affected by its presence in any way and is identical to voltammogram of pure electrolyte (Brdicka solution). In the case of antibody IgG bound onto PAMB a very low signal can be observed (Fig. 2C) and a slight increase of this signal height can be observed after attaching the second antibody IgY resulting to the PAMB-IgG-IgY formation (Fig. 2D). For this increase thiol moieties, which are present in the both antibodies and that provide analogous (but significantly lower) response like MT, are responsible. The evidence of MT binding on PAMB-IgG-IgY assembly is obvious from a significant increase of characteristic Cat2 peak (Fig. 2E).

Further experiments at constant concentration of the construct were performed with gradually increasing concentrations of MT. Based on the electrochemical measurement results it was found that the concentration of bound MT increases slower with the increasing concentrations of the applied MT. In the studied range of applied MT concentrations approximately fivefold increase of applied MT concentration result in app. twofold increase of bound MT only (Fig. 2F). The approximately twofold increase of bound MT represent the increase in the concentration values from 8.2 ng/mL to

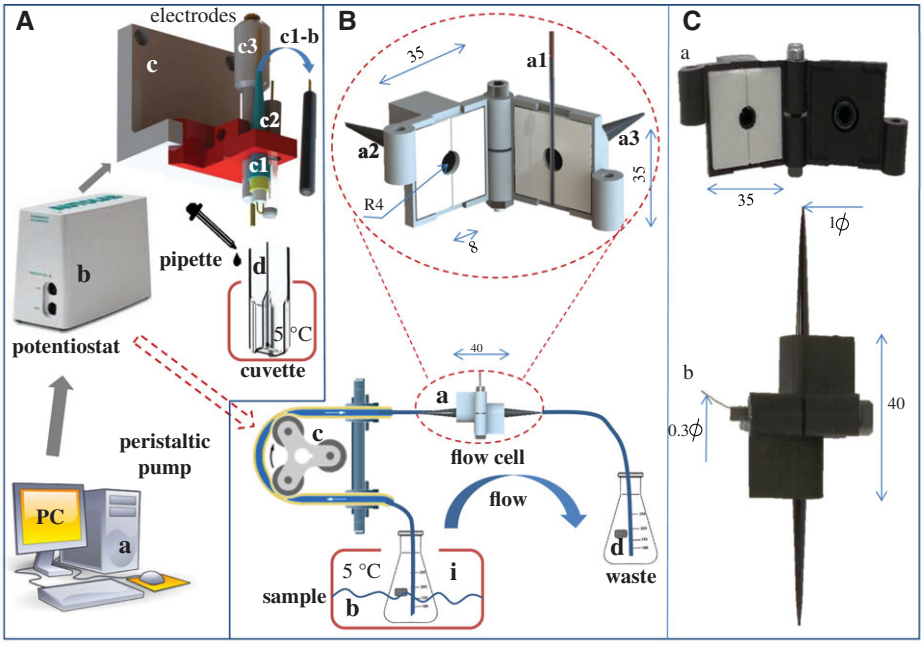

Figure 3. (A) Scheme of stationary electrochemical apparatus: (a) personal computer, (b) potentiostat (PGSTAT101), (c) three electrode wiring with holder printed by 3D printer: (c1) working electrode (Hg/Cu-WE) or glassy carbon (GCE-WE), (c2) reference electrode (Ag/AgCl/3 M KCl-RE), (c3) auxiliary electrode (Pt-CE), and (d) plastic cuvette tempered at 5°C. (B) Scheme of flow electrochemical apparatus: (a) flow cell printed by 3D printer, (a1) working electrode (Hg/Cu-WE), (a2) reference electrode (carbon tip –RE), (a3) auxiliary electrode (carbon tip – CE), (b) tempered sample at 5°C, (c) peristaltic pump, and (d) waste. (C) Photograph of flow cell (a) open and (b) closed.

19.0 ng/mL while the relative amount of bound MT decreases from 15.3% to 8.1% (related to the applied amount of MT). For verification of data obtained, determination of the residual concentration of unbound MT was estimated too. Evaluated concentrations of unbound MT correlates very well with the initially applied amount and with the amount of bound MT. It was not possible to evaluate very low concentrations of bonded MT quantitatively due to the sensitivity of the method used, therefore, data are presented from the applied concentration higher than 50 ng/mL. Results presented, however, sufficiently confirm the formation of PAMB-IgG-IgY-MT complex.

To determine concentrations of applied, bound, and unbound MT the calibration curve was determined using commercial MT standard. MT concentrations were changed from 3.9 to 125.6 ng/mL. Linear dependence was observed in whole range of used concentrations and dependence was as follows:

$$I\,(nA) = 1.1850\ c\,(ng/mL) - 7.0558,\ R^2 = 0.9930,\ n = 6. \quad (1)$$

Linear dependence of MT bound to the beads indicates that this immunoconstruct could be used in microfluidic device for MT capturing from the sample and magnetic manipulation.

3.2 Determination of working electrode for flow application (stationary phase)

Due to incompatibility of HMDE with microfluidic devices, two solid working electrodes (WE) were suggested for MT detection. The first one was GCE modified with mercury film (deposition at –0.9 V in 0.01 M $Hg(NO_3)_2$ solution). The second one was Cu wire covered with amalgam (Cu wire dipped into 0.01 M $Hg(NO_3)_2$ solution, Hg/Cu-WE). Both WE were characterized with respect to sensitivity, linear response, and surface stability. Further, a microfluidic device for flow detection of MT employing either modified GCE or Hg/Cu-WE was constructed. In stationary arrangement (Fig. 3A) the electrodes properties were optimized and then implemented to a flow system (Fig. 3B). The apparatus was controlled with computer (Fig. 3Aa), portable potentiostat (Fig. 3Ab), 3D printed electrodes holder (Fig. 3Ac) with working electrodes (Fig. 3Ac1a and Ac1b), reference argentochloride electrode (Fig. 3Ac2) and Pt auxiliary electrode (Fig. 3Ac3). In stationary arrangement 2.5 mL cuvette tempered as an electrochemical cell to 5°C was used (Fig. 3Ad) and the samples in volume of 10 μL were pipetted into the cell containing Brdicka electrolyte.

The voltammograms of Brdicka solution without MT and with 1 μg/mL MT on modified GCE-WE were recorded within potential range from –1.8 to –0.7 V (Fig 4A). In both cases the typical signals of cobalt (RS2Co) close to potential of –1.2 V were recorded. After application of MT to Brdicka solution, the signals Cat1 and Cat2 typical for HMDE could not be distinguished. Therefore, the intensity of the signal was taken from the position of –1.5 V as shown in Fig. 4A, red curve. Then, the influence of scan rate and deposition time on peaks positions and intensities was studied (Fig. 4B). With the increasing scan rate (0.0125–0.2 V/s) and deposition time (30–360 s) the intensity of Cat2 signal increased (Fig 4B, red and blue full curves). The position of RS2Co signal varied within interval –1.1 and –1.2 V (Fig. 4B red and blue dashed curve).

Hg/Cu-WE was tested analogically. First, the voltammograms of Brdicka electrolyte without MT and with 50 ng/mL MT within potential range from –1.8 to –0.7 V were recorded (Fig. 4C). At both curves the typical cobalt signals (RS2Co)

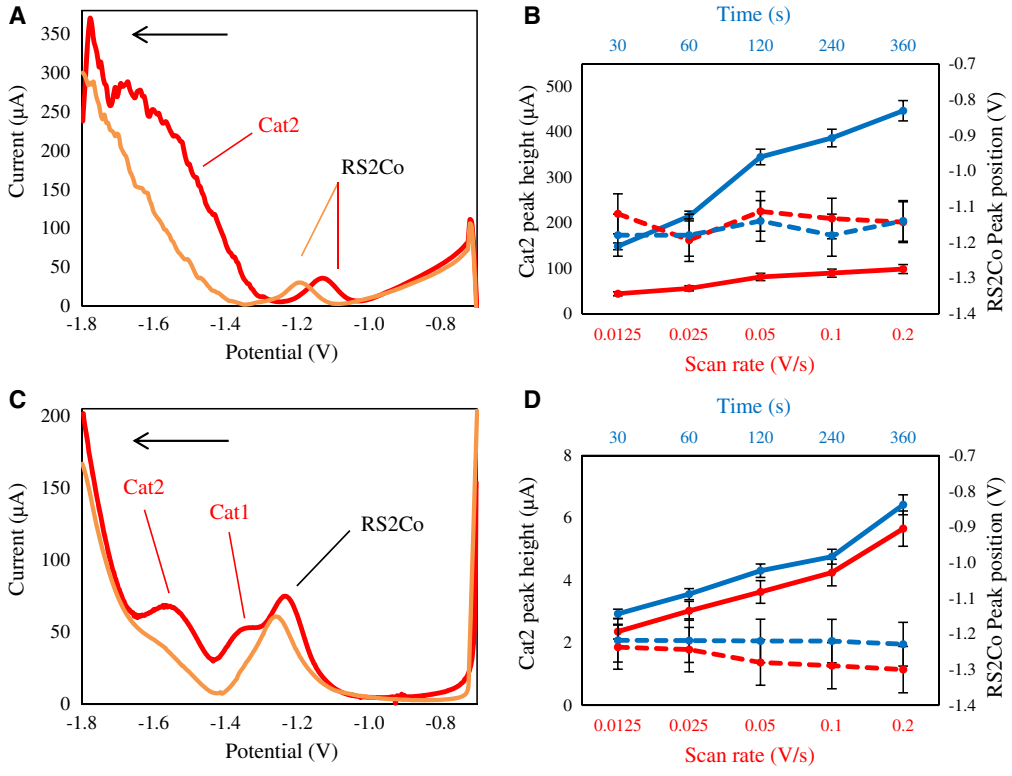

Figure 4. Differential pulse voltammetry of MT. (A) DP voltammograms of Brdicka solution (yellow line) and MT sample (red line) measured on GCE modified with a mercury layer. (B) Cat2 peak height (solid line) and RS2Co peak position (dashed line) dependence on scan rate value (red lines) and on deposition time (blue lines). ((C) DP voltammograms of Brdicka solution (yellow line) and MT sample (red line) measured on Hg/Cu-WE. (D) Cat2 peak height (single line) and RS2Co peak position (dashed line) dependence on scan rate value (red lines) and on deposition time (blue lines).

at potential of –1.2 V were detected, and well-developed Cat1 and Cat2 signals typical for MT on HMDE [55,56] were found in the presence of MT (Fig. 4C, red curve). Then, the influence of scan rate and deposition time on peaks positions and intensities were studied (Fig. 4D). With the increasing scan rate and deposition time the intensity of Cat 2 signal increased (Fig. 4D, full lines). The position of the signal RS2Co was within range from –1.2 to –1.3 V (Fig. 4D, dashed lines). The calibration curve in the concentration range 73–217 ng/mL exhibited regression equation $y = 0.0733x - 3.3264$ and determination coefficient $R^2 = 0.9942$. According to the obtained results, modified GCE was suitable for detection of higher MT concentrations incompatible with practical application and the voltammograms did not contain well developed Cat1 and Cat2 signals. The voltammograms were affected with high noise at potentials lower than –1.5 V caused by hydrogen development (observed as bubbles formation on GCE surface). This leads to decreased repeatability of the measurements and complicated evaluation of the signals. The modification of the GCE was shown to be instable and has to be renewed after each measurement. On the other hand, Hg/Cu-WE was found to be promising for intended microfluidic device. The measurements were well repeatable and Cat1 and Cat2 peaks positions on the voltammograms are in good agreement with HMDE records. The electrode surface was easily renewable by CV with broader potential range.

Hg/Cu electrode surface was further investigated using SEM and detailed view of element distribution on electrode surface was obtained by using SEM Elemental Mapping. It clearly follows from the obtained SEM results that the modified copper electrode surface is covered with formed amalgam in agreement with expected result (Fig. 5A and B).

3.3 Design and optimization of flow electrochemical device for detection of metallothionein

Hg/Cu-WE was implemented into flow electrochemical system (Fig. 3B). To the portable potentiostat controlled by computer a 3D-printed flow cell (Fig. 3Ba) containing the electrodes was connected. The flow cell was easy to disassemble and allowed a quick replacement of the electrodes. As working electrode Hg/Cu-WE was used (Fig. 3Ba1). Compared to stationary arrangement the surface of WE was 2.5-times smaller. As reference electrode (Fig. 3Ba2) and auxiliary electrode (Fig. 3Ba3) carbon tips were used. The sample was tempered to 5°C (Fig. 3Bb) and transferred to the cell by peristaltic pump (Fig. 3Bc) and after the measurement transferred to waste (Fig. 3Bd).

The voltammograms of Brdicka solution without and with 50 ng/mL MT are shown in Fig. 6A. As same as in the case of stationary arrangement all typical signals Cat1, Cat2, and RS2Co were observed. Decreasing of the electrode surface was manifested by proportional decreasing of the RS2Co signal. Then, peak area within potential range –0.7 to –1.7 V at different flow rates (0–1800 μL/min) were measured (Fig. 6B). It was observed that the height of the RS2Co peak increased with the increasing flow rate with maximum at 1200 μL/min, at higher flow rates a gradual decrease was observed. The position of the Cat2 signal was –1.25 V at all flow

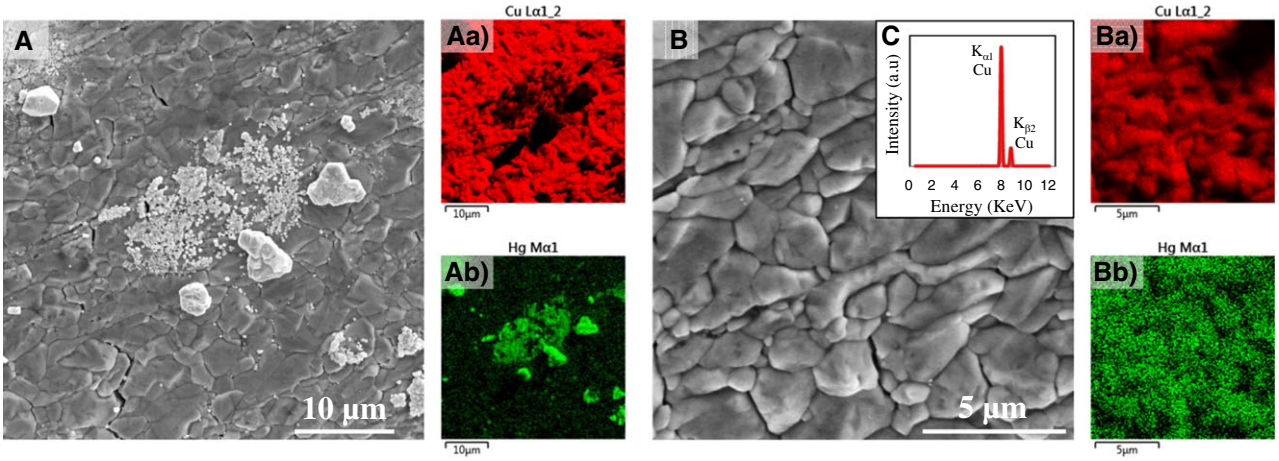

Figure 5. SEM micrographs of Hg/Cu electrode surface combined with SEM Elemental Mapping and X-ray fluorescence record of Cu wire used for Hg/Cu electrode. (A) Section with excess of mercury (particles in the central part of image) on surface slightly covered by copper amalgam (compare with Elemental Mapping images Aa and Ab). (B) Representative section of uniformly covered electrode surface with copper amalgam (compare with Elemental Mapping images Ba and Bb). (C) *X*-ray fluorescence record of Cu wire used for Hg/Cu electrode demonstrating the purity of material used.

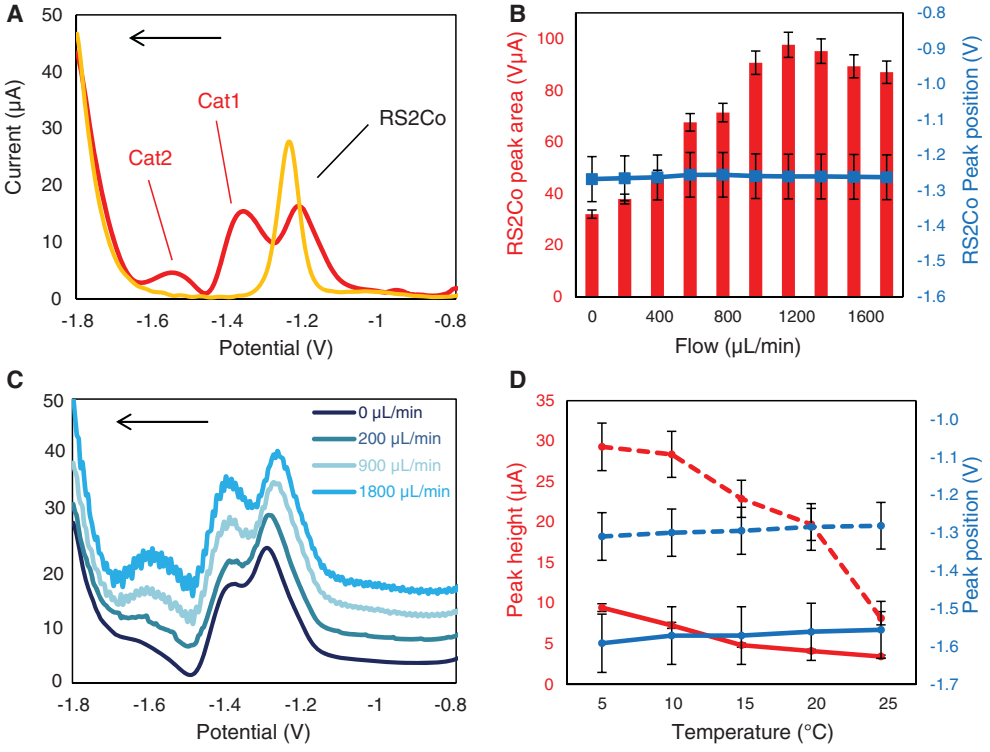

Figure 6. Detailed characteristic of Hg/Cu-WE in flow. (A) DP voltammograms of Brdicka solution (yellow line) and MT sample (red line) measured on Hg/Cu-WE in flow cell system (50 ng/mL MT at flow rate 400 µL/min). (B) Dependence of RS2Co peak area (red columns) and RS2Co peak position (blue line) on different flow rates (0-1800 µL/min). (C) The influence of DP voltammograms quality of 10 ng/mL MT solution on different flow rates (0-1800 µL/min). (D) Dependence of Cat2 (single line) and RS2Co (dashed line) peaks height (red lines) and position (blue lines) on temperature (150 ng/mL MT solution).

rates. Then, the noise was also studied with the increasing flow rate (Fig. 6C). It was observed that the height of both signals increases with increasing flow rate, but the noise increased too. The RS2Co and Cat2 peaks height was strongly dependent on temperature, whereas the highest signals were observed at 5°C (Fig. 6D red lines), which is consistent with previous findings [58]. Positions of RS2Co and Cat2 signals were with increasing temperature slightly shifted to positive potentials (Fig. 6D blue lines). The calibration curve in the concentration range 12.5–86 ng/mL exhibited regression equation $y = 0.0198x + 2.6323$ with determination coefficient $R^2 = 0.9858$. The possibility of the system integration, mobility, decreasing of analysis time, low samples, and reagents consumption, multiplexing and control of the reaction conditions belong to the main advantage of the microfluidic chips [60]. Detection possibilities of the microfluidic devices are comparable to common laboratory instruments [61]. Till now no microfluidic chip for detection of MT has been published. Due to the fluidic arrangement MT analysis can be miniaturized and implemented to "Lab On a Chip," which

Table 2. MT content in serum samples from patients with diagnosed spinocellular carcinoma (SCC), determined by fluidic electrochemical device

Patient	Sex	Age	Primary diagnosis	MT (μg/mL)[a)]	MT (μg/mL)[b)]
19	M	60	SCC, localization oropharynx	117	101
22	M	54	SCC	112	95
24	M	56	Basalioma, mucosal lesions	122	99

a) Determined by DPV with HMDE
b) Determined by developed fluidic device with electrochemical detection based on MT concentration bound in PAMB-IgG-IgY-MT complex.

have broad field of application in pharmaceutical, biochemical, and military industry [61] and allows point-of care testing in areas with lack of technical infrastructure.

3.4 Determination of MT in serum from patients with head and neck cancer

The utility of the device was tested on real samples of serum from patients suffering from spinocellular carcinoma. Blood serum is a standard and well-characterized sample used for MT determination by Brdicka reaction. The obtained results were compared with standard technique for MT determination [9]. The results are shown in Table 2. It is obvious that the obtained results were in good agreement with those measured by Brdicka reaction at HMDE. This slight discrepancy is generally observed when compared MT determination by Brdicka reaction and immunochemical methods [49].

4 Concluding remarks

In this work, super-paramagnetic agarose beads covalently coupled with recombinant protein A (PAMB) and two types of antibodies (IgG and IgY) were used. The complex (PAMB-IgG-IgY) was used for its specific ability to bound MT and this ability was successfully applied to real samples of patient with head and neck cancer. The Brdicka reaction was used for MT detection in flow system adapted to a microfluidic home-made printed 3D chip. The individual steps detecting stationary and flow phases were thoroughly optimized in this work. Method described in this contribution can be easily and cheaply implemented in "Lab On a Chip" and used for point-of-care testing or automation.

Financial support by SPINCANCER NT/14337 is highly acknowledged. The authors wish to express their special thanks to Dagmar Uhlirova for perfect technical assistance.

The authors declare no conflict of interests.

5 References

[1] Romero-Isart, N., Vasak, M., *J. Inorg. Biochem.* 2002, *88*, 388–396.

[2] Miles, A. T., Hawksworth, G. M., Beattie, J. H., Rodilla, V., *Crit. Rev. Biochem. Mol. Biol.* 2000, *35*, 35–70.

[3] Babula, P., Masarik, M., Adam, V., Eckschlager, T., Stiborova, M., Trnkova, L., Skutkova, H., Provaznik, I., Hubalek, J., Kizek, R., *Metallomics* 2012, *4*, 739–750.

[4] Krizkova, S., Ryvolova, M., Hrabeta, J., Adam, V., Stiborova, M., Eckschlager, T., Kizek, R., *Drug Metab. Rev.* 2012, *44*, 287–301.

[5] Coyle, P., Philcox, J. C., Carey, L. C., Rofe, A. M., *Cell. Mol. Life Sci.* 2002, *59*, 627–647.

[6] Zhang, J., Sun, R. J., Liu, Y., Wang, G. N., Wang, Q. L., *Iran J. Public Health* 2014, *43*, 696–704.

[7] Sochor, J., Hynek, D., Krejcova, L., Fabrik, I., Krizkova, S., Gumulec, J., Adam, V., Babula, P., Trnkova, L., Stiborova, M., Hubalek, J., Masarik, M., Binkova, H., Eckschlager, T., Kizek, R., *Int. J. Electrochem. Sci.* 2012, *7*, 2136–2152.

[8] Krizkova, S., Masarik, M., Majzlik, P., Kukacka, J., Kruseova, J., Adam, V., Prusa, R., Eckschlager, T., Stiborova, M., Kizek R., *Acta Biochim. Pol.* 2010, *57*, 561–566.

[9] Polanska, H., Raudenska, M., Gumulec, J., Sztalmachova, M., Adam, V., Kizek, R., Masarik, M., *Oral Oncol.* 2014, *50*, 168–177.

[10] Park, Y., Yu, E., *J. Gastroenterol. Hepatol.* 2013, *28*, 1565–1572.

[11] Eckschlager, T., Adam, V., Hrabeta, J., Figova, K., Kizek, R., *Curr. Protein Pept. Sci.* 2009, *10*, 360–375.

[12] Pekarik, V., Gumulec, J., Masarik, M., Kizek, R., Adam, V., *Curr. Med. Chem.* 2013, *20*, 534–544.

[13] Ruttkay-Nedecky, B., Nejdl, L., Gumulec, J., Zitka, O., Masarik, M., Eckschlager, T., Stiborova, M., Kizek, R., *Int. J. Mol. Sci.* 2013, *14*, 6044–6066.

[14] Gumulec, J., Adam, V., Kizek, R., Masarik, M., *PLoS One* 2014, *9*, 1–14.

[15] Zalewska, M., Trefon, J., Milnerowicz, H., *Proteomics* 2014, *14*, 1343–1356.

[16] Krizkova, S., Fabrik, I., Adam, V., Hrabeta, P., Eckschlager, T., Kizek, R., *Bratisl. Med. J.* 2009, *110*, 93–97.

[17] Adam, V., Fabrik, I., Eckschlager, T., Stiborova, M., Trnkova, L., Kizek, R., *TRAC-Trends Anal. Chem.* 2010, *29*, 409–418.

[18] Petrlova, J., Potesil, D., Mikelova, R., Blastik, O., Adam, V., Trnkova, L., Jelen, F., Prusa, R., Kukacka, J., Kizek, R., *Electrochim. Acta* 2006, *51*, 5112–5119.

[19] Raspor, B., *J. Electroanal. Chem.* 2001, *503*, 159–162.

[20] Raspor, B., Paic, M., Erk, M., *Talanta* 2001, *55*, 109–115.

[21] Adam, V., Petrlova, J., Wang, J., Eckschlager, T., Trnkova, L., Kizek, R., *PLoS One* 2010, *5*, e11441, 11441–11448.

[22] Sobrova, P., Vyslouzilova, L., Stepankova, O., Ryvolova, M., Anyz, J., Trnkova, L., Adam, V., Hubalek, J., Kizek, R., *PLoS One* 2012, *7*, e49654.

[23] Novotny, L., Yosypchuk, B., *Chem. Listy* 2000, *94*, 1118–1120.

[24] Mikkelsen, O., Schroder, K. H., *Analyst* 2000, *125*, 2163–2165.

[25] Mikkelsen, O., Schroder, K., *Anal. Lett.* 2000, *33*, 3253–3269.

[26] Mikkelsen, O., Schroder, K. H., *Electroanalysis* 2001, *13*, 687–692.

[27] Fadrna, R., Cahova-Kucharikova, K., Havran, L., Yosypchuk, B., Fojta, M., *Electroanalysis* 2005, *17*, 452–459.

[28] Mikkelsen, O., Schroder, K. H., Aarhaug, T. A., *Collect. Czech. Chem. Commun.* 2001, *66*, 465–472.

[29] Mikkelsen, O., Schroder, K. H., *Anal. Chim. Acta* 2002, *458*, 249–256.

[30] Mikkelsen, O., Skogvold, S. M., Schroder, K. H., Gjerde, M. I., Aarhaug, T. A., *Anal. Bioanal. Chem.* 2003, *377*, 322–326.

[31] Mikkelsen, O., Nordhei, C., Skogvold, S. M., Schrøder, K. H., *Anal. Lett.* 2004, *37*, 2925–2936.

[32] Mikkelsen, O., vanden Berg, C. M. G., Schroder, K. H., *Electroanalysis* 2006, *18*, 35–43.

[33] Fadrna, R., *Anal. Lett.* 2004, *37*, 3255–3270.

[34] Fadrna, R., Yosypchuk, B., Fojta, M., Navratil, T., Novotny, L., *Anal. Lett.* 2004, *37*, 399–413.

[35] Kim, N., Son, S. H., Kim, W. Y., *Sens. Actuator B-Chem.* 2014, *198*, 157–163.

[36] Kim, N., Son, S. H., Kim, C. T., Cho, Y. J., Kim, C. T., Kim, W. Y., *Sens. Actuator B Chem.* 2011, *157*, 627–634.

[37] Kim, N., Shon, S. H., Kim, C. T., Cho, Y. J., Kim, C. J., *Curr. Appl. Phys.* 2011, *11*, 1210–1214.

[38] Qian, Q. M., Wang, Y. S., Yang, H. X., Xue, J. H., Liu, L., Zhou, B., Wang, J. C., Yin, J. C., Wang, Y. S., *Anal. Biochem.* 2013, *436*, 45–52.

[39] Capdevila, M., Gonzalez-Bellavista, A., Munoz, M., Atrian, S., Fabregas, E., *Chem. Commun.* 2010, *46*, 2040–2042.

[40] Chen, M., Zhao, C. F., Chen, W., Weng, S. H., Liu, A. L., Liu, Q. C., Zheng, Z. F., Lin, J. H., Lin, X. H., *Analyst* 2013, *138*, 7341–7346.

[41] Lin, C. C., Wang, J. H., Wu, H. W., Lee, G. B., *Jala* 2010, *15*, 253–274.

[42] Ng, A. H. C., Uddayasankar, U., Wheeler, A. R., *Anal. Bioanal. Chem.* 2010, *397*, 991–1007.

[43] Tarn, M. D., Pamme, N., *Expert Rev. Mol. Diagn.* 2011, *11*, 711–720.

[44] Tekin, H. C., Gijs, M. A. M., *Lab Chip* 2013, *13*, 4711–4739.

[45] vanReenen, A., deJong, A. M., den Toonder, J. M. J., Prins, M. W. J., *Lab Chip* 2014, *14*, 1966–1986.

[46] Trnkova, L., Krizkova, S., Adam, V., Hubalek, J., Kizek, R., *Biosens. Bioelectron.* 2011, *26*, 2201–2207.

[47] Skalickova, S., Zitka, O., Nejdl, L., Krizkova, S., Sochor, J., Janu, L., Ryvolova, M., Hynek, D., Zidkova, J., Zidek, V., Adam, V., Kizek, R., *Chromatographia* 2013, *76*, 345–353.

[48] Krizkova, S., Adam, V., Eckschlager, T., Kizek, R., *Electrophoresis* 2009, *30*, 3726–3735.

[49] Krizkova, S., Blahova, P., Nakielna, J., Fabrik, I., Adam, V., Eckschlager, T., Beklova, M., Svobodova, Z., Horak, V., Kizek, R., *Electroanalysis* 2009, *21*, 2575–2583.

[50] Laemmli, U. K., *Nature* 1970, *227*, 680–685.

[51] Tmejova, K., Hynek, D., Kopel, P., Krizkova, S., Blazkova, I., Trnkova, L., Adam, V., Kizek, R., *Colloid Surf. B Biointerfaces* 2014, *117*, 534–537.

[52] Hunziker, P. E., Kaur, P., Wan, M., Kanzig, A., *Biochem. J.* 1995, *306*, 265–270.

[53] Krizkova, S., Adam, V., Kizek, R., *Electrophoresis* 2009, *30*, 4029–4033.

[54] Adam, V., Baloun, J., Fabrik, I., Trnkova, L., Kizek, R., *Sensors* 2008, *8*, 2293–2305.

[55] Adam, V., Blastik, O., Krizkova, S., Lubal, P., Kukacka, J., Prusa, R., Kizek, R., *Chem. Listy* 2008, *102*, 51–58.

[56] Fabrik, I., Ruferova, Z., Hilscherova, K., Adam, V., Trnkova, L., Kizek, R., *Sensors* 2008, *8*, 4081–4094.

[57] Ryvolova, M., Krizkova, S., Adam, V., Beklova, M., Trnkova, L., Hubalek, J., Kizek, R., *Curr. Anal. Chem.* 2011, *7*, 243–261.

[58] Hynek, D., Tmejova, K., Trnkova, L., Hubalek, J. et al., in: Yuki Saito, Tatumi Kikuchi (Eds.), *Voltammetry: Theory, Types and Applications*, Nova Science Publishers, Inc., New York 2013, pp. 145–170.

[59] Adam, V., Krizkova, S., Zitka, O., Trnkova, L., Petrlova, J., Beklova, M., Kizek, R., *Electroanalysis* 2007, *19*, 339–347.

[60] Mirasoli, M., Guardigli, M., Michelini, E., Roda, A., *J. Pharm. Biomed. Anal.* 2014, *87*, 36–52.

[61] Nugen, S. R., Asiello, P. J., Connelly, J. T., Baeumner, A. J., *Biosens. Bioelectron.* 2009, *24*, 2428–2433.

[62] Stejskal, K., Krizkova, S., Adam, V., Sures, B., Trnkova, L., Zehnalek, J., Hubalek, J., Beklova, M., Hanustiak, P., Svobodova, Z., Horna, A., Kizek, R., *IEEE Sens. J.* 2008, *8*, 1578–1585.

[63] Briseno, A. L., Song, F. Y., Baca, A. J., Zhou, F. M., *J. Electroanal. Chem.* 2001, *513*, 16–24.

[64] Sestakova, I., Kopanica, M., Havran, L., Palecek, E., *Electroanalysis* 2000, *12*, 100–104.

[65] Fabrik, I., Krizkova, S., Huska, D., Adam, V., Hubalek, J., Trnkova, L., Eckschlager, T., Kukacka, J., Prusa, R., Kizek, R., *Electroanalysis* 2008, *20*, 1521–1532.

